arXiv:1903.03506v1 [cond-mat.stat-mech] 8 Mar 2019

Unsupervised identification of the phase transition on the 2D-Ising model

Constantia Alexandrou[a,b] **Andreas Athenodorou**[a] **Charalambos Chrysostomou**[a] **Srijit Paul**[a]

[a] *Computation-based Science and Technology Research Center, The Cyprus Institute, 20 Kavafi Str., Nicosia 2121, Cyprus.*

[b] *University of Cyprus, 1 Panepistimiou Avenue 2109 Aglantzia, Nicosia.*

E-mail: c.alexandrou@cyi.ac.cy, a.athenodorou@cyi.ac.cy, c.charalambous@cyi.ac.cy, s.paul@cyi.ac.cy

Abstract: We investigate deep learning autoencoders for the unsupervised recognition of phase transitions in physical systems formulated on a lattice. We use spin configurations produced for the 2-dimensional ferromagnetic Ising model in zero external magnetic field. We study numerically the relation between one latent dimension extracted from the autoencoder to the critical temperature T_c. The autoencoder reveals the two phases, one for which the spins are ordered and the other for which spins are disordered, reflecting the restoration of the $\mathbb{Z}_2$ symmetry as the temperature increases. For the largest volume studied, the transition between the two phases occurs very close to the theoretically extracted critical temperature. We define as a quasi-order parameter the absolute average latent dimension $\tilde{z}$, which enables us to predict the critical temperature. We show that one can build the latent susceptibility and use it to quantify the value of the critical temperature $T_c(L)$ at different lattice sizes and that these values suffer from only small finite scaling effects. We demonstrate that $T_c(L)$ extrapolates to the known theoretical value as $L \to \infty$ suggesting that the autoencoder can also be used to extract the critical temperature of the phase transition to an adequate precision.

Contents

1 Introduction **1**

2 The Ferromagnetic 2-Dimensional Ising Model **2**
- 2.1 Swendsen-Wang algorithm 3
- 2.2 Monte-Carlo simulation setup 3
- 2.3 Phase structure, observables and order parameters 4

3 Deep Learning Autoencoders **4**
- 3.1 Proposed Autoencoder Model 5

4 Results **7**
- 4.1 The latent dimension per configuration 7
- 4.2 The absolute average latent dimension 10
- 4.3 The Latent Susceptibility and the Critical Temperature 13

5 Conclusions and Outlook **15**

1 Introduction

Recent advances in the implementation of Artificial Intelligence (AI) for physical systems, especially, on those which can be formulated on a lattice, appear to be suitable for observing the corresponding underlying phase structure [1–16]. So far methods such as the Principal Component Analysis (PCA) [2, 3, 7, 17], Supervised Machine Learning [4, 11, 18] (ML) as well as autoencoders [6, 7] appear to successfully identify different phase regions of classical statistical systems, such as the 2-dimensional (2D) Ising model that describes the ferromagnetic-paramagnetic transition. These techniques were also applied on quantum statistical systems, such as the Hubbard model [5] that describes the transition between conducting and insulating systems. Very recently, similar studies have been applied for simulations of quantum fields on the lattice, such as the $SU(2)$ gauge theory [19] with an increased complexity in the data due to the structure of the $SU(2)$ gauge group.

Trained neural networks can thus help distinguish phases in simple statistical systems the structure of which is known, but more importantly in more complex systems where the underlying phase structure is unknown. In this work, we would like to examine whether the proposed, fully-connected (Dense), deep learning autoencoder, which does not require supervised training, can shed light on the phase structure of the 2D-Ising model. Deep learning autoencoders are frequently used in cases where data hides interesting structure by processing the raw datasets. They can, therefore, be used to discover interesting structure in ensembles produced for a range of a parameter that characterizes the phase space of

the model in different sectors with different physical properties. One such example is the ferromagnetic Ising model for which at the critical temperature T_c, the system undergoes a transition from the ordered phase to the disordered.

In this work, we investigate the action of unsupervised machine learning, namely the deep learning autoencoder (not variational), towards the identification of the phase transition of the 2D-Ising model. More specifically, we produce decorrelated configurations for the 2D-Ising model for a given range of temperatures and then we apply the autoencoder trying to understand what information of the phase structure we can capture. Hence, technically, this work combines the production of configurations using Monte Carlo methods as well as the deep learning autoencoder algorithm. We observe that the autoencoder can capture the underlying $\mathbb{Z}_2$ symmetry and can indeed find out where the transition occurs by identifying as a relevant quasi-order parameter the mean value of the absolute latent dimension. Although this quantity is not suitable for predicting the order of the transition, it can determine the critical temperature with small finite scaling effects.

This article is organised as follows: In section 2 we present a brief description of the 2D-Ising model, explaining the production of the configurations as well as its phase structure. In section 3 we discuss the deep learning autoencoder, explain how it works and provide the structure of the network. Subsequently, in section 4 we provide our results, and finally, in section 5, we conclude.

2 The Ferromagnetic 2-Dimensional Ising Model

One of the most interesting physical phenomena in nature is magnetism. It is known that the ferromagnetic materials exhibit a spontaneous magnetisation in the absence of an external magnetic field. Such magnetisation occurs only if the temperature of the system is lower than a known critical temperature T_c, the so called Curie temperature. If the temperature of the system is raised so that $T > T_c$, then the magnetisation vanishes. In principle, the critical temperature T_c separates the microstates of the system from being ordered or magnetised for $T < T_c$ to being randomly oriented resulting in zero magnetisation; these two phases correspond to the ferromagnetic and the disordered phases, respectively.

Ferro-magnetism has a quantum mechanical nature and, thus, a lot of effort is invested towards its understanding. Albeit quantum mechanical, simple classical models can help to gain insight into this effect. The 2D-Ising model is a classical model that is commonly used to study magnetisation. The 2D-Ising model can be considered as a lattice with $N = N_x \times N_y$ sites, on each of which a double valued spin s_i is located, either being in an "up" orientation denoted by $\uparrow$ or $s_i = +$ or "down" denoted by $\downarrow$ or $s_i = -$.

The macroscopic properties of the 2D-Ising system are determined by the nature of the accessible micro-states. Thus, it is useful to know the dependence of the Hamiltonian on the spin configurations. The total energy is given by

$$H = -J \sum_{i,j=nn(i)}^{N} s_i s_j - \mu h \sum_{i=1}^{N} s_i \,, \tag{2.1}$$

where J is the self-interaction between neighbouring spins, h the external magnetic field and μ is the atomic magnetic moment. Note that in the first sum, the notation $nn(i)$ represents nearest-neighbour pairs; the sum is taken over all nearest-neighbouring pairs.

In the case of the canonical ensemble, in other words, when the system is attached to a thermal reservoir and kept at a constant temperature T, as the time passes the spins are left to fluctuate with rates depending on the reservoir's temperature. This behaviour can be captured in a Monte Carlo (MC) simulation in the canonical ensemble. For $T = 0$ the system is frozen with all spins being at one direction either down or up. The orientation of the spins is arbitrary, however, the dynamics enforce the system to choose one of the two directions. This corresponds to the spontaneous symmetry breaking of the $\mathbb{Z}_2$ global symmetry group. Although the Hamiltonian of the system is invariant under $\mathbb{Z}_2$ transformations, the degenerate ground states are not invariant but get interchanged under such transformations.

For small finite values of the temperature of the system, spins still form large sectors where all spins are correlated and point to one direction. Above the critical temperature T_c, the spins are disordered and $\mathbb{Z}_2$ symmetry is restored.

The question that we address in this work is whether the behaviour described above can be captured by a deep learning autoencoder when we pass it ensembles for a sequence of temperatures separated by some δT. More precisely, we seek to understand if a qualitative description of the phase structure of the Ising model can be extracted and whether one can determine the critical temperature T_c.

2.1 Swendsen-Wang algorithm

The MC simulation for the 2D-Ising model is conventionally performed using the Metropolis algorithm. Since this algorithm is based on local updates, near the critical temperature where the correlation length diverges, it faces the problem of critical slowing down. In order to tackle this problem, we have implemented the Swendsen-Wang cluster algorithm [20, 21], which is based on global updates of the spin configurations. This algorithm relies on the formation of bonds between every pair of nearest neighbours(ij) that are aligned at a given temperature T, with a probability $p_{ij} = 1 - \exp(-2\beta J)$, where $\beta = \frac{1}{k_B T}$ ($k_B \equiv$ Boltzmann constant). A single cluster is defined as all the spins, which are connected via bonds. The global update is defined as the collective flipping with a probability of $1/2$, on all the spins in each cluster [22, 23]. This step works because of the so-called Fortuin-Kasteleyn mapping of the Ising model on the random-cluster model. Thus, global updates enable us to produce equilibrium configurations close to the T_c with a few thermalisation steps.

2.2 Monte-Carlo simulation setup

In this work we chose to investigate the case of zero external magnetic field ($h = 0$) and for simplicity we have set $J = 1$ and $k_B = 1$. In this case, the theoretically calculated value of the critical temperature is

$$T_c = \frac{2}{\ln\left(1+\sqrt{2}\right)} = 2.269185\,. \tag{2.2}$$

To extract experimentally this quantity one has to investigate the order parameter of theory, namely the magnetization. The first question that we address is whether we can get an approximate estimate of this temperature by using unsupervised learning. To this purpose, we choose a sequence of different values of temperature, and for each one, we start from a frozen configuration of spins, perform a large enough number of thermalisation sweeps and then save the configuration. For every single temperature, we repeat the procedure 200 times.

2.3 Phase structure, observables and order parameters

The phase structure of the 2D-Ising model can be reduced to the study of the magnetic order of the system [24, 25]. If we suppose that there are $N_\uparrow$ spins pointing upwards and $N_\downarrow$ spins pointing downwards, then the total magnetic moment would be $N_\uparrow - N_\downarrow$ ($\mu = 1$). The largest possible magnetic moment would, therefore, be N. Thus, we can define the magnetic order parameter or magnetization per spin configuration naturally as:

$$m = (N_\uparrow - N_\downarrow)/N\,, \tag{2.3}$$

while the average magnetization $M = \langle m \rangle$. M can get values between -1 and 1, and the average of the absolute magnetization $\tilde{m} = \langle |m| \rangle$ is just the magnetic order. Hence, if $\tilde{m}$ is close to 0, then the system is highly disordered and, thus, not magnetised, with approximately half of the spins pointing up and the other half pointing down. On the other hand, if $\tilde{m}$ is approximately 1, the system is ordered and, thus, magnetised with nearly all the spins pointing in the same direction.

The point $T = T_c$ is called the *critical point* and separates the ordered $T < T_c$ phase and disordered $T > T_c$ phase. At $T = T_c$ the system is described by a second order phase transition, i.e. *à la* Ehrenfest [26] the first derivative of the free energy with respect to the external field which is the order parameter is continuous while the second derivative of the free energy is discontinuous.

3 Deep Learning Autoencoders

Autoencoders is a variety of artificial neural networks utilized for learning data codings in an unsupervised manner, efficiently [27, 28]. An autoencoder aims to define a representation (encoding) for an assemblage of data, usually performing dimensionality reduction. An autoencoder encodes the input data ($\{X\}$) from the input layer into a latent dimension ($\{z\}$), and then uncompresses that latent dimension into an approximation of the original data ($\{\,X\}$). This drives the autoencoder to engage in dimensionality reduction, by learning how to ignore the noise and recognise significant characteristics of the input data. The first layer of an autoencoder might learn to encode simple, identifiable and local features, and the second layer by using the output of the first layer learns to encode more complex and less local features, until the final layer of the encoder learns to identify and encode the most complex and global characteristics of the input data. As Fig. 1 shows, an autoencoder

consists of two components, the encoder function g_ϕ and a decoder function f_θ and the reconstructed input is $X = f_\theta(g_\phi(x))$.

In the training phase, the autoencoder learns the parameters ϕ and θ together, where $f_\theta(g_\phi(x))$ can approximate an identity function. Various metrics can be used to measure the error between the original input X and the reconstruction $\tilde{X}$, but the most simple and most commonly used is the Mean Square Error (MSE) as this is provided in Eq. 3.1, where n_{data} is the number of data points:

$$MSE(\theta, \phi) = \frac{1}{n_{\text{data}}} \sum_{i=1}^{n_{\text{data}}} (X_i - f_\theta(g_\phi(X_i)))^2 \,. \tag{3.1}$$

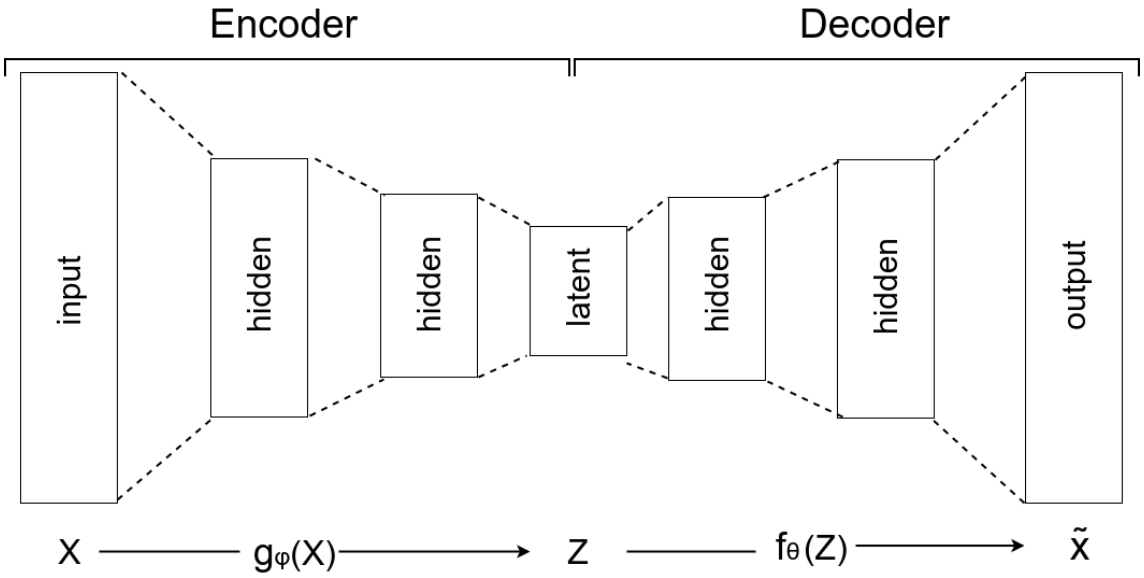

Figure 1. Basic structure of an autoencoder

3.1 Proposed Autoencoder Model

For the analysis of the proposed method, an eight-layer, fully connected (Dense), autoencoder is proposed, as Fig. 2 shows, where the encoder compresses the configurations into a single latent dimension. Through experimentation, we determine that the best model to detect the transition consists of the encoder with the input layer, first, second and third hidden layers having 625, 256, 64 and 1 neurons, respectively. The activation function used is relu, as shown in Eq. 3.2, for all layers except the third hidden layer, where tanh was used, as shown in Eq. 3.3. For the decoder, the first, second and third hidden layers use 64, 256, and 625 neurons, respectively. For the output layers, the number of neurons is set to be equal to the number of values in the configuration under investigation. The activation function used is relu, as given in Eq. 3.2, for all hidden layers, and for the output layer, tanh is used, as per Eq. 3.3.

$$\text{relu} : y = max(0, x) = \left\{ \begin{array}{l} x, \text{ if } x > 0 \\ 0 \quad \text{if } x \leq 0 \end{array} \right\} . \tag{3.2}$$

$$\tanh : y = \frac{1 - e^{-2x}}{1 + e^{-2x}} \, . \tag{3.3}$$

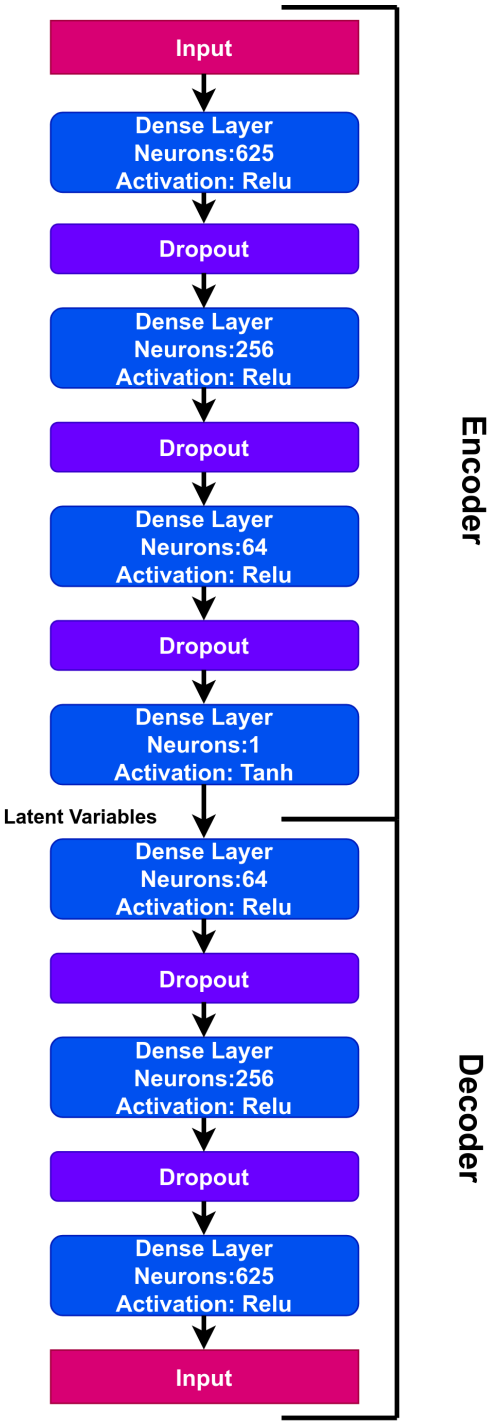

Figure 2. Proposed autoencoder model in the standard Machine Learning nomenclature.

For the proposed autoencoder model we use the so-called dropout realization technique [29]. The dropout regularization technique refers to dropping out neurons from each layer, randomly, when training. Dropout is successfully used for reducing over-fitting in neural networks by preventing complex co-adaptations on training data. For the training of the proposed autoencoder model the data are split into training (66.66...%) and testing (33.33...%) sets, and the training is performed for 2000 iterations. The implementation was performed using Keras [30] and Tensorflow [31].

4 Results

4.1 The latent dimension per configuration

Each configuration is re-expressed in the form of a vector, and then it is read as an input by the autoencoder. One can think of the input as a column with entries of 1 and -1, placed in some lexicographic order and having a length equal to L^2. More precisely, for each different lattice size $L = N_x = N_y$ we feed to the network all the configurations produced for all different temperatures, and we extract the latent dimension $z_{i_{\rm conf}}$. In other words, each configuration is assigned a number, the latent dimension, which includes all the physically necessary information so that the decoder re-creates the actual configuration. It should be made clear that configurations for different lattice volumes have been fed separately into the autoencoder, i.e. the autoencoder receives information for only one lattice volume, and thus, it "knows" nothing about configurations produced for other volume sizes.

In order to identify signals of the phase structure of the 2D-Ising model, as a first step, we investigate how the latent dimension $z_{i_{\rm conf}}$ behaves as a function of the temperature T for each configuration. We produce 40000 configurations, namely 200 configurations for every single temperature. The produced configurations are for 200 different values of temperatures within the range $T = 1 - 4.5$ and separated by $\delta T = 0.0175$. We make sure that we cover the whole range of temperatures between the two extreme cases of the Ising behaviour, the nearly "frozen" at $T \simeq 1$, and the complete disordered $T \simeq 4.5$. Furthermore, we assume that we have no prior knowledge on what is happening in between these two extremes. We note that we could choose different temperature ranges that cover all possible phase regions; for instance, we could choose instead $T = 0.01 - 1000$ with $\delta T = 0.01$, but of course the computational effort would be much more significant.

In Fig. 3 we show the latent dimension for each different configuration, as a function of the temperature T, for four different lattice sizes, $L = 25, 35, 50, 150$.

Fig. 3 has the following features:

- For low temperatures we obtain two plateaus, one located at $z = 1$ and one at $z = -1$. A first simplistic explanation for this pattern would be that it corresponds to two distinct states that are not connected through any kind of transformation. This reflects the spontaneously broken $\mathbb{Z}_2 \equiv \{-1, 1\}$ global symmetry group. One can interpret these two plateaus as the two cases where all spins are up or down. This interpretation is confirmed by the results presented in Fig. 4 where we show the absolute correlation coefficient $C_{z,m}$ between the latent dimension z and the magnetisation m defined as

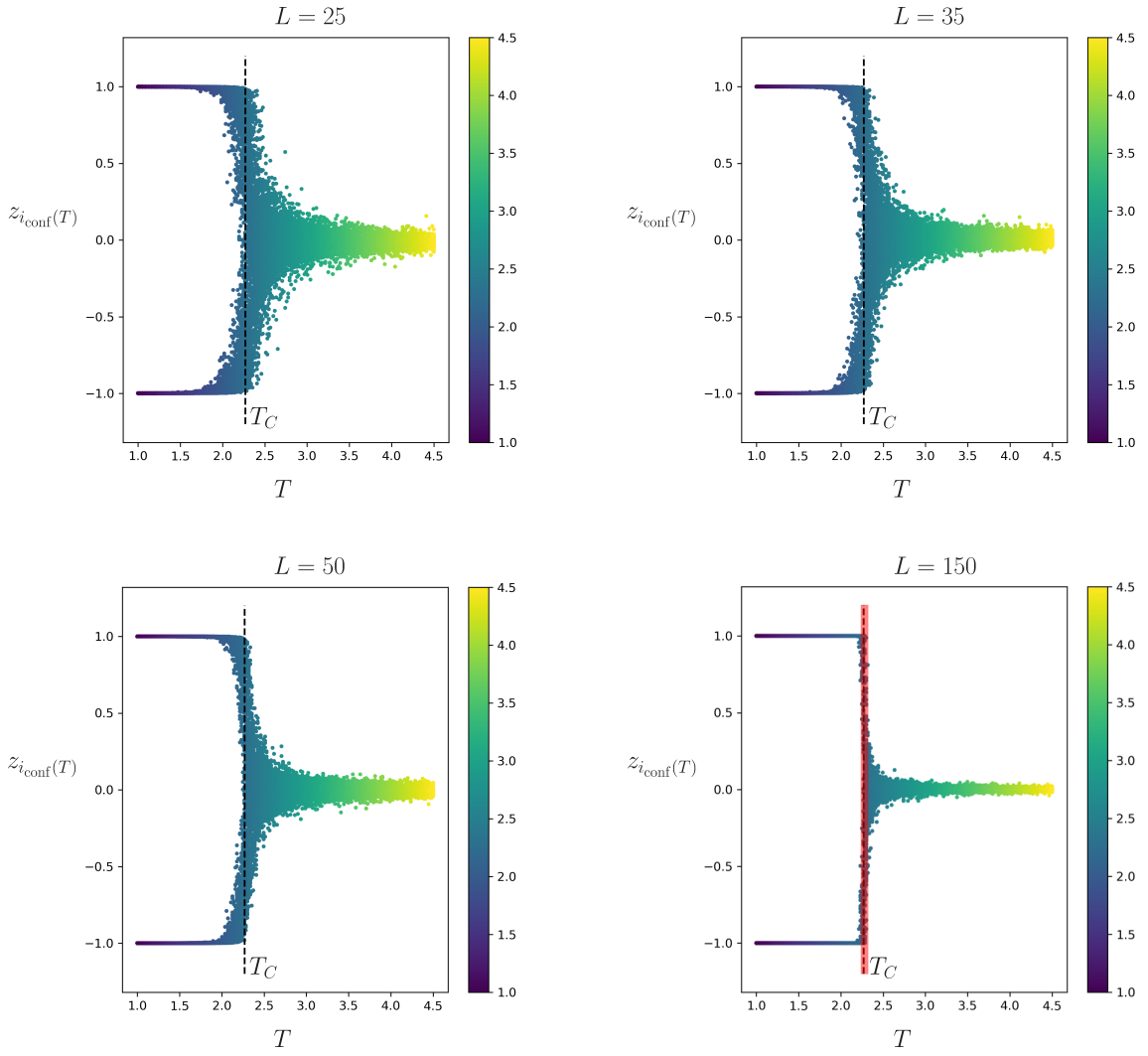

Figure 3. The latent dimension for each configuration as a function of the temperature for four different lattice volumes. The dashed line represents the analytically extracted value of the critical temperature (Eq. 2.2). The red shaded area in the plot for $L = 150$ is the region where (by fitting to a constant) we expect to find the $T_c(L = 150)$. The color on the gradient illustrator on the right denotes the temperature T.

$$C_{z,m} = \frac{\langle (z - \bar{z})(m - \bar{m}) \rangle}{\sqrt{\langle (z - \bar{z})^2 \rangle \langle (m - \bar{m})^2 \rangle}} \,. \tag{4.1}$$

The fact that at low temperatures the absolute correlation coefficient is 1 demonstrates that the two different values of the latent dimension -1 and 1 correspond to the two orientations of the spins. Finally, the two plateaus become more distinct as the lattice size increases.

- At some temperature range ΔT_{trans} the aforementioned behaviour collapses to one state, which is located around $z = 0$. This reflects the restoration of $\mathbb{Z}_2$ symmetry.

In other words, it corresponds to the case where all the spins are disoriented.

- There is a critical point where there is a change in the pattern. As the lattice size increases the width of this transition decreases with $\Delta T_{\text{trans}} \to 0$ and this step becomes steeper and steeper. At $L \to \infty$ the transition is localised right on the critical temperature T_c extracted analytically.

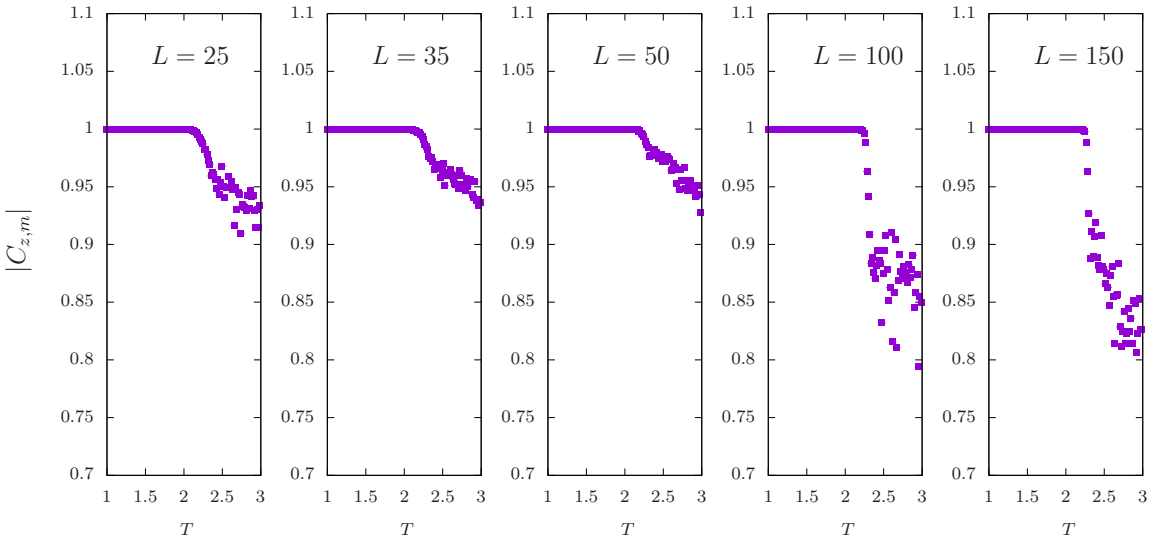

Figure 4. The absolute correlation coefficient defined in Eq. 4.1 as a function of the temperature for the five different lattice sizes.

Evidently, plotting the latent dimension as a function of the temperature demonstrates that the autoencoder predicts the two phases. Also, it provides to a good approximation the critical temperature. In fact from Fig. 3 the transition appears to occur right at the critical temperature for $L = 150$. By fitting the points of the latent dimension which, to a good approximation, behave linearly to a constant as a function of T we can restrict that the collapse of the two states located at 1 and -1 occurs at $T \simeq 2.28(4)$. This temporal region is denoted in Fig. 3 as the shaded area in red. In Fig. 4 we observe that within this temporal region the value of the absolute correlation coefficient $C_{z,m}$ starts to decrease from 1. This demonstrates that, although highly correlated, the latent dimension and magnetisation are two different quantities.

Finally, we observed that for low temperatures the latent dimension is, in a good approximation, equally distributed between the values of $z = 1$ and $z = -1$. This can be seen in Fig. 5 where we present the average latent dimension $\langle z \rangle$ for each temperature and $L = 150$ as a function of the temperature.

One could also investigate what happens within different "temperature windows" introducing, however, a degree of supervision. For instance, we can use a temperature window within the range $T = 1 - 2$ and apply the autoencoder. The outcome would be the behaviour presented in the left panel of Fig. 6, where only the two ordered states are visible without the presence of a critical point. Since there is no visible signal for a phase transition

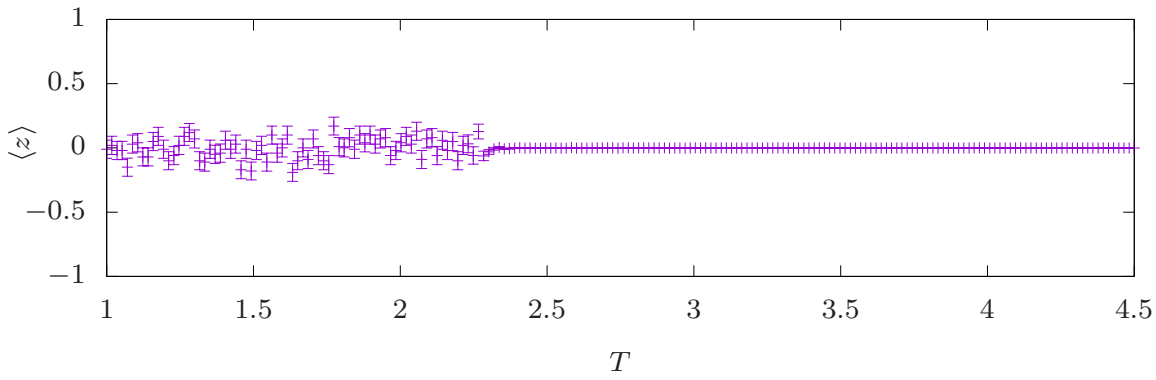

Figure 5. The average latent dimension $\langle z \rangle$ as a function of the temperature T for $L = 150$.

behaviour within this range of T it is reasonable to use another temperature window. If we choose $T = 3 - 4.5$, for instance, the corresponding latent dimension would be the one given on the right panel of Fig. 6 where no particular pattern is observed. A sensible next step would be to investigate what happens within a range of temperatures located between the two previous temperature windows, for instance $T = 1 - 4$.

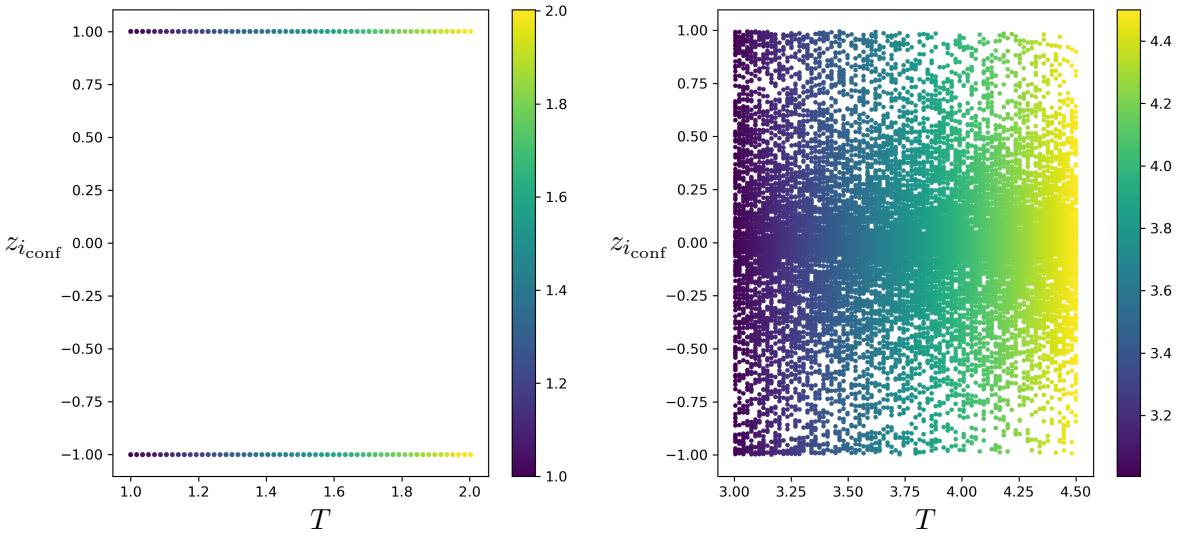

Figure 6. The latent dimension for each configuration as a function of the temperature for $L = 100$, obtained by applying the autoencoder on configurations produced within the range of temperatures $T = 1 - 2$ (left) and $T = 3 - 4.5$ (right).

4.2 The absolute average latent dimension

Since the latent dimension per configuration is symmetric with respect to the T axis, it would be reasonable to define the average absolute latent dimension as a parameter indi-

cating the phase as

$$\tilde{z} = \frac{1}{N_{\rm conf}} \sum_{i=1}^{N_{\rm conf}} |z_{i_{\rm conf}}| \ . \tag{4.2}$$

Fig. 3 shows that the latent dimension resembles the behaviour of the magnetization per spin configuration as a function of the temperature. The absolute average magnetization defines the order parameter of the system distinguishing the two different phases. For the case of the autoencoder we can define an additional quasi-order parameter as the absolute average latent dimension.

In the left-hand-side of Fig. 7 we provide the magnetisation as a function of the temperature while on the right-hand side we provide the absolute latent dimension. Indeed the absolute latent dimension looks similar to the magnetisation, albeit becoming steeper as the lattice size increases. Clearly, the magnetization behaves as an order parameter with the characteristics of a second order phase transition while the absolute latent dimension is consistent with a first order phase transition. We can, therefore, conclude that the absolute average latent dimension can be used as an order parameter to identify the critical temperature, but cannot capture the right order of the phase transition. The fact that $\tilde{z}$ as a function of the temperature becomes steeper as the lattice size increases suggests that the critical temperature $T_c(L)$ as a function of the lattice size L extracted from the autoencoder data will suffer less from finite-size scaling effects as discussed in detail in Section 4.3.

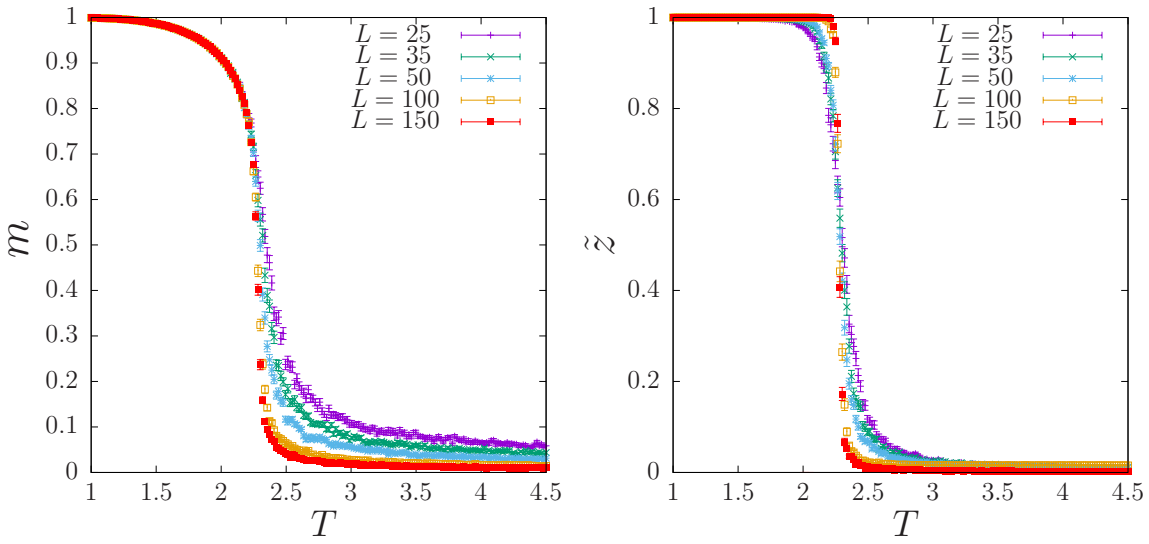

Figure 7. The average latent dimension as a function of the temperature for five different lattice volumes.

Traditionally, $T_c(L)$ can be extracted by probing the peak of the magnetic susceptibility χ at zero magnetic field h, where

$$\chi = \frac{L^2}{T} \left(\langle m^2 \rangle - \langle m \rangle^2 \right) \ . \tag{4.3}$$

According to finite size scaling theory, close enough to T_c, magnetic susceptibility χ scales as

$$\chi \propto (t)^{-\gamma} \ , \tag{4.4}$$

where $t = (T - T_c)/T_c$ is the reduced temperature and $\gamma = 7/4$ a critical exponent [24]. The magnetic susceptibility measures the ability of a spin to respond due to a change in the external magnetic field. In the same manner we define the *latent susceptibility* as

$$\chi_{\tilde{z}} = \frac{L^2}{T} \left(\langle \tilde{z}^2 \rangle - \langle \tilde{z} \rangle^2 \right) \ . \tag{4.5}$$

For the extraction of T_c one realizes, by looking at Fig. 7, that more data points close to the critical behaviour are needed to extract the critical temperature from the latent susceptibility. Hence, we produce configurations for a grid of temperatures near the critical regime. More specifically, we produce 200 configurations per temperature, for 200 different values of T in the range of $T = 2 - 2.8$ and $\delta T = 0.004$ for all the volumes considered. In addition, for $L = 100$ and $L = 150$ we produce 200 configuration for each value of T, in the range of $T = 2.22 - 2.34$ with $\delta T = 0.0006$. These new configurations, however, are not used to train the autoencoder. Instead, we use the synaptic weights extracted and predict the latent dimension for the new configurations. Hence, this serves as a confirmation that our data do not suffer from over-fitting.

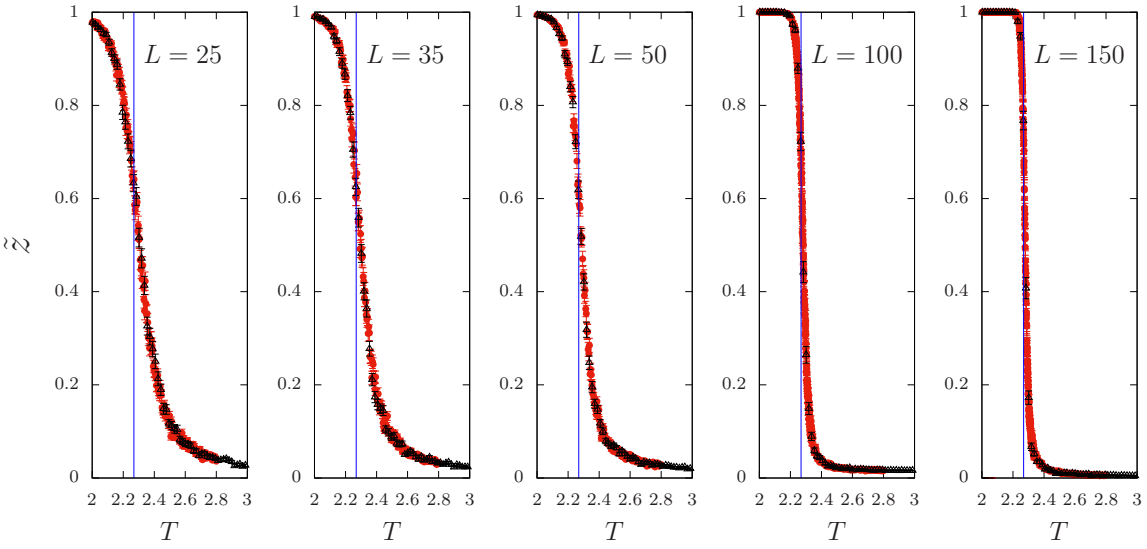

Figure 8. The red points show the predicted latent dimension for the configurations produced around the critical point T_c while in black the latent dimension extracted in the first set of configurations on which we have trained the encoder. The blue vertical line corresponds to the analytically extracted critical temperature T_c.

In Fig. 8 we present the results of applying the autoencoder weights on the new configurations produced in the region close to the critical point. We compare with results extracted using configurations produced in the range $T = 1 - 4.5$. Both datasets agree, and

there is a nice continuation of the behaviour of the absolute average latent dimension within the critical regime. This demonstrates that the execution of the encoder does not suffer from any over-fitting occurrence and at the same time more data points can be used for the extraction of $\chi_{\tilde{z}}$. Furthermore, the plot for $L = 150$, behaves nearly as a step function with the step being right on the theoretically extracted T_c. By fitting the second moment of the latent dimension, as this is described in section 4.3, one sees that the transition occurs at $T_c(L = 150) = 2.2779(3)$; this value is very close to the theoretically extracted value $T_c = 2.26918$.

In the following section we present the analysis of our data in order to investigate the latent susceptibility $\chi_{\tilde{z}}$ and, to subsequently, extract the critical temperature $T_c(L)$ from the corresponding peak.

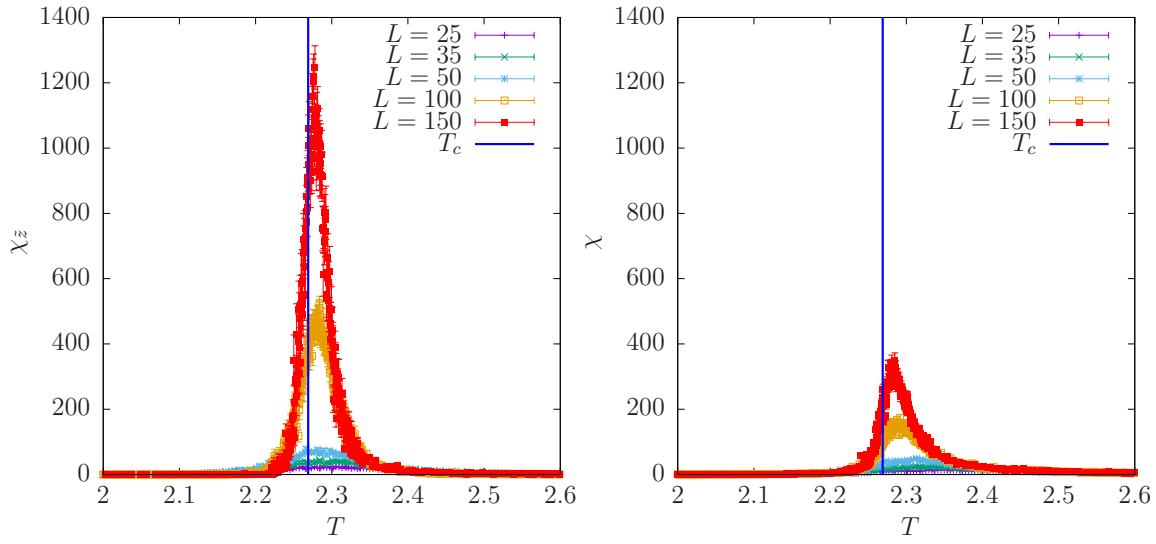

Figure 9. The latent susceptibility (left) and magnetic susceptibility (right) as a function of the temperature for five different lattice volumes. The blue vertical line denotes the analytically extracted value for the critical temperature (Eq. 2.2).

4.3 The Latent Susceptibility and the Critical Temperature

In the previous sections, we provided strong evidence that the latent dimension, resulting from the proposed autoencoder, demonstrates the underlying phase transition and that it can also be used as a rough estimate for the critical temperature T_c. Nevertheless, as the finite lattice size L increases we need to make sure that $T_c(L)$ tends to the right limit i.e. it convergences to the theoretically extracted value given in Eq. 2.2 as $L \to \infty$.

To investigate the convergence of $T_c(L)$, we first extract $T_c(L)$ for each different lattice size and then extrapolate to infinite L. $T_c(L)$ can be extracted by probing the peak of the latent susceptibility for each L. The latent susceptibility as a function of the temperature for the five different lattice sizes is presented on the left-hand side of Fig. 9. Unlike the magnetic susceptibility, presented on the right-hand side of Fig. 9, the latent susceptibility

is much sharper with peaks being closer to the known critical temperature T_c. This means that the critical temperature for each L is influenced by less finite-size scaling effects.

Our temporal grid is fine enough and enables an adequate extraction of the $T_c(L)$ from the coordinates of Fig. 9. Hence, there is no need to use multi-histogram reweighting [16] techniques. The latent dimension behaves to a large extent as a step function, and thus, tends to $\propto \delta(T - T_c)$ as $L \to \infty$. In addition, the derivative of the latent susceptibility appears to be continuous. So we can also use a Gaussian fit to estimate the critical temperature.

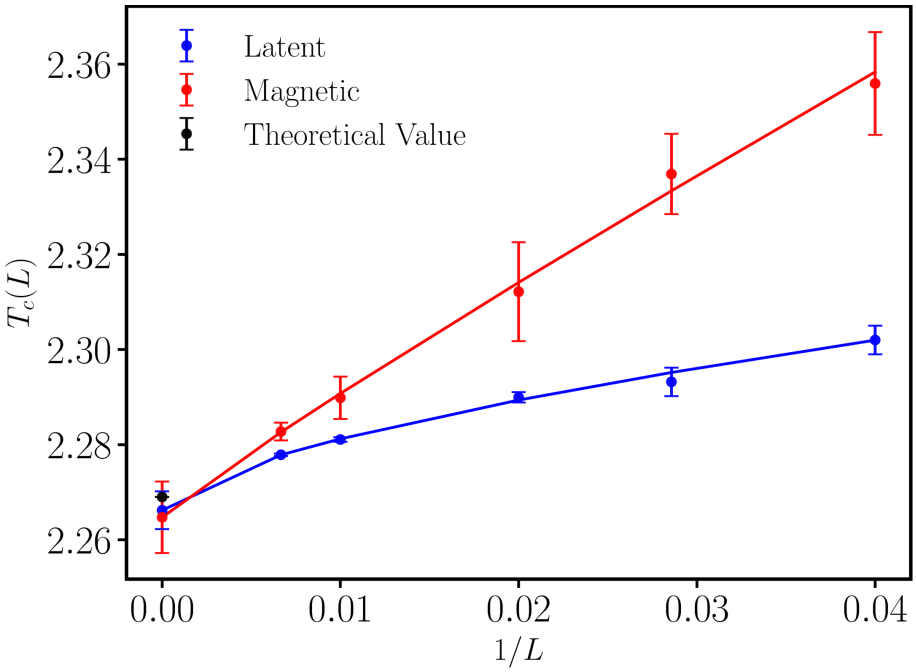

Figure 10. The critical temperature $T_c(L)$ extracted from fitting the magnetic (red) and the latent (blue) susceptibilities as a function of $1/L$ to Eq. 4.6.

In Fig. 10 we present $T_c(L)$ extracted from fitting the latent susceptibility and the magnetic susceptibility as a function of $1/L$. Results obtained using the latent susceptibility suffer less from finite-size scaling effects as compared to those when using the magnetic susceptibility. Adopting, the usual finite-size scaling behaviour

$$T_c(L) - T_c(L = \infty) \propto L^{-1/\nu}\,, \tag{4.6}$$

we fit both susceptibilities to the ansatz $T_c(L) = T_c(L = \infty) + \alpha L^{-1/\nu}$. Our findings are listed in Table 1.

Susceptibility	$T_c(L=\infty)$	ν	χ^2/dof
Magnetic	2.265(8)	1.08(20)	0.15
Latent	2.266(4)	1.60(14)	0.41

Table 1. The results for $T_c(L=\infty)$ and ν extracted by fitting the magnetic as well as the latent susceptibilities to the ansatz $T_c(L) = T_c(L=\infty) + \alpha L^{-1/\nu}$.

As expected, fitting the data for $T_c(L)$ resulting from the magnetic susceptibility yields values of $T_c(L=\infty)$ and ν which are consistent with the analytically extracted values $T_c = 2.269184$ and $\nu = 1$. Turning now to the case of the latent dimension, it appears that the results of $T_c(L)$ when fitted with a form of the known scaling behaviour of Eq. 4.6, yield a value for $T_c(L=\infty)$, which is in accordance with the theoretical expectation. This provides a good evidence that the deep learning autoencoder does not only predict the phase regimes of the 2D-Ising model as well as give an estimate for the critical temperature, but can also lead to a precise evaluation of the critical temperature.

5 Conclusions and Outlook

In this work, we apply a deep learning auto-encoder on configurations produced for the 2D Ferromagnetic Ising model for performing a classification in an unsupervised manner. Hence, with no prior knowledge on the system, we demonstrate that we can predict the phase structure of this system qualitatively as well as quantitatively by determining both phase regions and the critical temperature.

At low temperatures, by making use of the latent dimension per configuration, the autoencoder predicts two states reflecting to the broken $\mathbb{Z}_2$ symmetry. As the temperature increases, these two states appear to collapse at one state, located around zero, and the underlying symmetry is restored. This behaviour becomes more distinct as the volume of the lattice increases and the point where the two states collapse is getting more and more local; this corresponds to the critical point of the phase transition.

One can define the average absolute latent dimension $\tilde{z}$ that displays partially the characteristics of an order parameter; namely, it can identify the phase but cannot capture the order of the phase. Although it resembles the behaviour of the magnetization it becomes steeper as the size of the volume increases, tending to a step function. The second moment of the absolute latent dimension defines a susceptibility, named latent susceptibility, the peak of which can determine the critical temperature $T_c(L)$. By extrapolating the values of $T_c(L)$ to $L \to \infty$ for the sequence of lattice sizes $L = 25,\ 35,\ 50,\ 100,\ 150$, we obtain for $T_c(L=\infty) = 2.266(4)$ in agreement with the exact value of $T_c = 2.26918$ calculated analytically. This suggests that the proposed deep learning (fully-connected) autoencoder can identify, in an unsupervised manner, the phase structure of the 2D-Ising model but can also lead to a precise extraction of the critical temperature at the limit of the infinite volume. As shown in Fig. 10 the values of $T_c(L)$ suffer with less finite size effects compared to those usually extracted by using the peak of the magnetic susceptibility, and one would

thus expect that the autoencoder could give a more precise prediction for T_c. Of course to test this hypothesis we need to extract $T_c(L)$ for larger volumes, for instance up to $L = 1024$ similarly to Ref. [16], and obtain the extrapolated value of $T_c(L = \infty)$. This requires the usage of a different autoencoder with more layers since memory limitations make the current autoencoder insufficient to work. This is a future extension of this work.

There are other several related directions in which this work can be extended. Since our proposed autoencoder has been tested just in one system, it would be important to investigate its generalisation to other physical systems with non-trivial phase structure. An important question, which could be answered is whether this neural network is capable of identifying the phases for cases in which an order parameter is either not known or not existing; such an example is the Hubbard model [32] describing the transition between conducting and insulating systems. Another relevant question is how the autoencoder behaves in cases where the phase transition is of a different order or an infinite order such as in the 2D XY spin model where the relevant phase transition is the Kosterlitz-Thouless which is of infinite order [33]. Finally, our future plans involve the testing of the autoencoder as a tool for the unsupervised extraction of the phase structure of physical systems with continuous symmetries. These involve quantum field theories formulated on the lattice such as the 3D ϕ^4 with $O(2)$ symmetry [34] where the phase transition is of second order and belongs to the same universality class as the 2D-Ising model, the 3D $U(1)$ gauge theory [35] for which the phase transition is of infinite order and belongs to the same universality class as the 2D XY model, as well as the 3D $SU(N)$ gauge theory [36] which has a second-order phase transition for $N \leq 3$, a weakly first order for $N = 4$ and first order for $N \geq 5$.

Acknowledgements

We would like to thank Giannis Koutsou, Nikos Savva, Spyros Sotiriadis, Mike Teper and Savvas Zafeiropoulos for fruitful discussions. We would also like to express our gratitude to Barak Bringoltz, Biagio Lucini and Davide Vadacchino for performing a critical reading of the manuscript. AA was financially supported by the Horizon 2020 of the European Commission research and innovation programmes VI-SEEM under grant agreement No 675121 as well as the OpenSESAME under grand agreement No 730943. CC also acknowledges support from the OpenSESAME project. SP is supported by the Horizon 2020 of the European Commission research and innovation programmes HPC-LEAP under the Marie Skłodowska Curie grant agreement No. 642069 and PRACE-5IP under grant agreement No 730913.

References

[1] J. Carrasquilla and R. G. Melko, *Machine learning phases of matter*, *Nature Physics* **13** (Feb, 2017) 431 EP –, [arXiv:1605.01735].

[2] E. van Nieuwenburg, Y.-H. Liu, and S. Huber, *Learning phase transitions by confusion*, *Nature Physics* **13** (Feb, 2017) 435 EP –, [arXiv:1610.02048].

[3] L. Wang, *Discovering phase transitions with unsupervised learning*, *Phys. Rev. B* **94** (Nov, 2016) 195105, [arXiv:1606.00318].

[4] P. Broecker, J. Carrasquilla, R. G. Melko, and S. Trebst, *Machine learning quantum phases of matter beyond the fermion sign problem*, *Scientific Reports* **7** (2017), no. 1 8823, [arXiv:1608.07848].

[5] K. Ch'ng, J. Carrasquilla, R. G. Melko, and E. Khatami, *Machine learning phases of strongly correlated fermions*, *Physical Review X* **7** (2017), no. 3 031038, [arXiv:1609.02552].

[6] S. J. Wetzel, *Unsupervised learning of phase transitions: From principal component analysis to variational autoencoders*, *Phys. Rev. E* **96** (Aug, 2017) 022140, [arXiv:1703.02435].

[7] W. Hu, R. R. P. Singh, and R. T. Scalettar, *Discovering phases, phase transitions, and crossovers through unsupervised machine learning: A critical examination*, *Phys. Rev. E* **95** (Jun, 2017) 062122, [arXiv:1704.00080].

[8] P. Broecker, F. F. Assaad, and S. Trebst, *Quantum phase recognition via unsupervised machine learning*, *arXiv e-prints* (July, 2017) arXiv:1707.00663, [arXiv:1707.00663].

[9] N. Yoshioka, Y. Akagi, and H. Katsura, *Learning disordered topological phases by statistical recovery of symmetry*, *Phys. Rev. B* **97** (May, 2018) 205110, [arXiv:1709.05790].

[10] J. Venderley, V. Khemani, and E.-A. Kim, *Machine learning out-of-equilibrium phases of matter*, *Phys. Rev. Lett.* **120** (Jun, 2018) 257204, [arXiv:1711.00020].

[11] W. Zhang, J. Liu, and T.-C. Wei, *Machine learning of phase transitions in the percolation and XY models*, *arXiv e-prints* (Apr., 2018) arXiv:1804.02709, [arXiv:1804.02709].

[12] R. B. Jadrich, B. A. Lindquist, and T. M. Truskett, *Unsupervised machine learning for detection of phase transitions in off-lattice systems. I. Foundations*, *jcp* **149** (Nov., 2018) 194109, [arXiv:1808.00084].

[13] D. Kim and D.-H. Kim, *Smallest neural network to learn the ising criticality*, *Phys. Rev. E* **98** (Aug, 2018) 022138, [arXiv:1804.02171].

[14] X. L. Zhao and L. B. Fu, *Machine Learning Phase Transition: An Iterative Proposal*, *arXiv e-prints* (Aug., 2018) arXiv:1808.01731, [arXiv:1808.01731].

[15] K. Kashiwa, Y. Kikuchi, and A. Tomiya, *Phase transition encoded in neural network*, arXiv:1812.01522.

[16] C. Giannetti, B. Lucini, and D. Vadacchino, *Machine Learning as a universal tool for quantitative investigations of phase transition*, arXiv:1812.06726.

[17] S. J. Wetzel, *Unsupervised learning of phase transitions: From principal component analysis to variational autoencoders*, *Physical Review E* **96** (2017), no. 2 022140, [arXiv:1703.02435].

[18] A. Morningstar and R. G. Melko, *Deep learning the ising model near criticality*, arXiv:1708.04622.

[19] S. J. Wetzel and M. Scherzer, *Machine Learning of Explicit Order Parameters: From the Ising Model to SU(2) Lattice Gauge Theory*, *Phys. Rev.* **B96** (2017), no. 18 184410, [arXiv:1705.05582].

[20] R. H. Swendsen and J.-S. Wang, *Nonuniversal critical dynamics in Monte Carlo simulations*, *Phys. Rev. Lett.* **58** (1987) 86–88.

[21] J.-S. Wang and R. H. Swendsen, *Cluster monte carlo algorithms*, *Physica A: Statistical Mechanics and its Applications* **167** (1990), no. 3 565 – 579.

[22] P. W. Kasteleyn and C. M. Fortuin, *Phase Transitions in Lattice Systems with Random Local Properties*, *Physical Society of Japan Journal Supplement, Vol. 26. Proceedings of the*

International Conference on Statistical Mechanics held 9-14 September, 1968 in Koyto., p.11 **26** (1969) 11.

[23] C. M. Fortuin and P. W. Kasteleyn, *On the Random cluster model. 1. Introduction and relation to other models*, *Physica* **57** (1972) 536–564.

[24] J. Cardy, *Scaling and Renormalization in Statistical Physics*. Cambridge Lecture Notes in Physics. Cambridge University Press, 1996.

[25] H. Gould, J. Tobochnik, and W. Christian, *An introduction to computer simulation methods*, vol. 1.

[26] G. Jaeger, *The ehrenfest classification of phase transitions: introduction and evolution*, *Archive for history of exact sciences* **53** (1998), no. 1 51–81.

[27] P. Vincent, H. Larochelle, Y. Bengio, and P.-A. Manzagol, *Extracting and composing robust features with denoising autoencoders*, in *Proceedings of the 25th international conference on Machine learning*, pp. 1096–1103, ACM, 2008.

[28] P. Vincent, H. Larochelle, I. Lajoie, Y. Bengio, and P.-A. Manzagol, *Stacked denoising autoencoders: Learning useful representations in a deep network with a local denoising criterion*, *Journal of machine learning research* **11** (2010), no. Dec 3371–3408.

[29] G. E. Hinton, N. Srivastava, A. Krizhevsky, I. Sutskever, and R. R. Salakhutdinov, *Improving neural networks by preventing co-adaptation of feature detectors*, arXiv:1207.0580.

[30] F. Chollet et al., "Keras." https://keras.io, 2015.

[31] M. Abadi, P. Barham, J. Chen, Z. Chen, A. Davis, J. Dean, M. Devin, S. Ghemawat, G. Irving, M. Isard, et al., *Tensorflow: a system for large-scale machine learning.*, in *OSDI*, vol. 16, pp. 265–283, 2016.

[32] J. Hubbard, *Electron Correlations in Narrow Energy Bands*, *Proceedings of the Royal Society of London Series A* **276** (Nov., 1963) 238–257.

[33] J. M. Kosterlitz and D. J. Thouless, *Ordering, metastability and phase transitions in two-dimensional systems*, *J. Phys.* **C6** (1973) 1181–1203. [,349(1973)].

[34] P. B. Arnold and G. D. Moore, *Monte Carlo simulation of O(2) ϕ^4 field theory in three-dimensions*, *Phys. Rev.* **E64** (2001) 066113, [cond-mat/0103227]. [Erratum: Phys. Rev.E68,049902(2003)].

[35] A. Athenodorou and M. Teper, *On the spectrum and string tension of U(1) lattice gauge theory in 2 + 1 dimensions*, *JHEP* **01** (2019) 063, [arXiv:1811.06280].

[36] J. Liddle and M. Teper, *The Deconfining phase transition in D=2+1 SU(N) gauge theories*, arXiv:0803.2128.